Propagation of nonlinear waves on an electron-charged surface of liquid helium

K. Mima* and H. Ikezi
Bell Laboratories, Murray Hill, New Jersey 07974
(Received 28 November 1977)

A theoretical study of the nonlinear behavior of the surface wave (or ripplon) propagating on the electron-charged surface of liquid helium is presented. The evolution of the wave packet is described by the nonlinear Schrödinger equation, and the wave is found to be either stable or unstable with respect to an amplitude perturbation depending on the choice of the wave number. Envelope solitons are formed in the one-dimensional case. In two dimensions it is found that wave packets collapse when the envelope contains large wave numbers, so that the surface tension determines wave evolutions; the physical dimension of the packet shrinks and the amplitude increases. The system we consider in this paper is suitable for experimental studies of solitons and collapse phenomena because the dissipation in liquid helium is small and the ripplon dispersion relation can be easily modified by an external electric field.

I. INTRODUCTION

The nonlinear behavior of a dispersive wave has been subjected to considerable theoretical attention.[1] It is well known that one of the remarkable properties of such waves is the existence of stationary wave pulses or packets called "solitons" which exist because of the dynamical balance between dispersion and nonlinear effects. Computational studies have found many interesting properties of such solitons. For instance, solitons are very stable and keep their identity against disturbances.[2] In many cases, a sinusoidal wave breaks into solitons and the original waveform is recovered after interactions with other solitons.[3] Two solitons often behave as if they were bound to each other.[4] On the other hand, recent studies of two- and three-dimensional systems have disclosed that the wave packet may collapse, i.e., shrink, rather than form stable solitons.[5,6]

The formation of one-dimensional solitons has been observed as excitations in several systems[7] including liquid water and low-temperature gaseous plasmas, and in nonlinear transmission lines. Experimental observations of the long-time behavior of solitons are, however, limited because of dissipation and the finite extent of the experimental systems. We would like to explore a new system which may bypass these difficulties.

Recently there has been a great deal of interest in a system consisting of a layer of electrons on the surface of liquid helium. The geometry of the system is sketched in Fig. 1. The wave propagating on the surface of the liquid, called "ripplon," has the following remarkable features: (i) the damping rate of the waves is very small because of the small viscosity in liquid helium, and (ii) the dispersion relation of the ripplons is controllable by changing the external static electric field applied to bind the electrons to the surface of the liquid. In particular, the group velocity v_g vanishes at particular wave numbers indicating that the wave packet will not propagate out of the system. These properties should enable us to experimentally study the long-time behavior of the nonlinear ripplon.

When the depth of the liquid z_0 is much greater than the wavelength, the linear dispersion relation of the ripplon of frequency ω_k as a function of the wave number k, is given by[8]

$$\omega_k^2 = \left(\rho g - \frac{(2\pi\sigma_0)^2 + E_0^2}{2\pi}\,|k| + \alpha k^2\right)\frac{|k|}{\rho} \quad . \tag{1}$$

Here, ρ is the density of the liquid, g the gravity constant, α the surface tension, σ_0 the equilibrium surface-electron charge density, and E_0

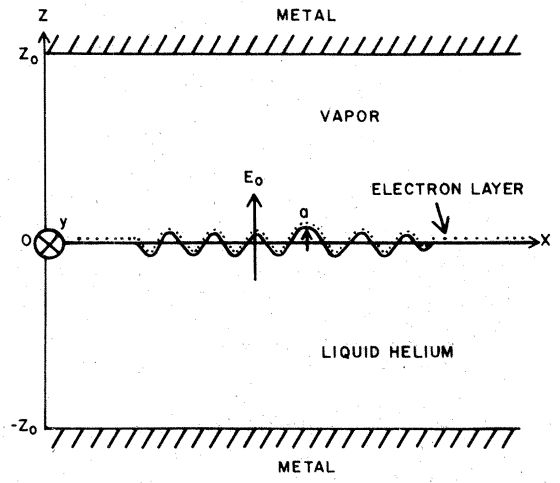

FIG. 1. Schematic of the electron-charged surface of a liquid-helium system.

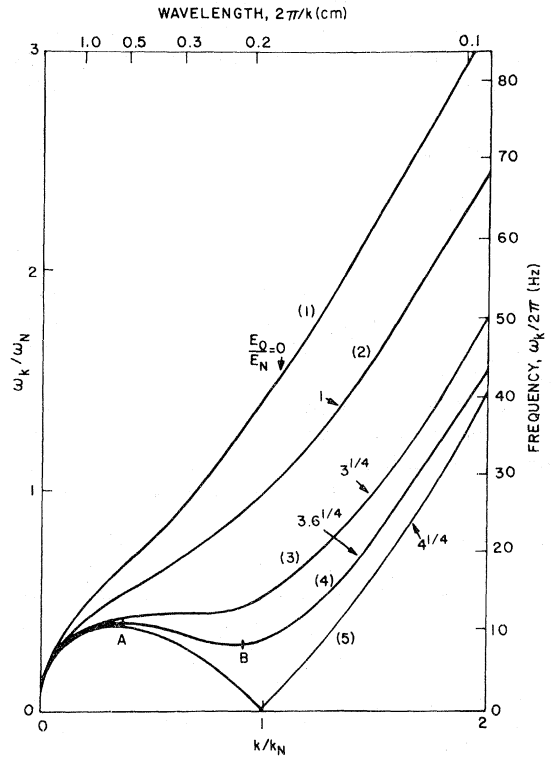

FIG. 2. Dispersion relation of the wave at different values of the electric field E_0. The normalizing factors ω_N, k_N, and E_N are defined by Eq. (42). $\omega_N/2\pi = 28$ Hz, $2\pi/k_N = 0.19$ cm, and $E_N = 1.5$ kV/cm when the temperature of liquid helium is 4.2°K.

the external electric field in the z direction (perpendicular to the liquid surface). Coordinates x and y are along the liquid surface. Depending on E_0, three types of dispersion curves are obtained as depicted in Fig. 2. Consider the waves propagating in the positive x direction. Although v_g is always positive when

$$E_0^2 < \pi(12g\rho\alpha)^{1/2} - (2\pi\sigma_0)^2$$

(see curve 1), we have two points A and B (see curve 4), where $v_g = 0$ when

$$\pi(12g\rho\alpha)^{1/2} < E_0^2 + (2\pi\sigma_0)^{1/2} < \pi(16g\rho\alpha)^{1/2} .$$

If

$$E_0^2 > \pi(16\rho g\alpha)^{1/2} - (2\pi\sigma_0)^2 ,$$

Then the Rayleigh-Taylor instability[9] grows because ω_k^2 becomes negative near $k = (\rho g/\alpha)^{1/2}$. When $k \gg (\rho g/\alpha)^{1/2}$, the surface-tension effects dominate over the gravity and electric-force effects, and the dispersion relation is given by $\omega_k^2 = \alpha k^3/\rho$.

In Sec. II, we consider a quasimonochromatic one-dimensional wave with a corresponding surface deformation of the form

$$a(x,t) = A(x,t)\exp(ikx - i\omega t) . \tag{2}$$

Here $\omega(>0)$ and $k(>0)$ are the carrier frequency and wave number. The amplitude and the phase of the wave are given by the slowly varying function $A(x,t)$. We will show that, except for a few particular combinations of E_0 and k, the evolution of A is described by

$$i\frac{\partial A}{\partial t} + iv_g\frac{\partial A}{\partial x} + \frac{1}{2}v_g'\frac{\partial^2 A}{\partial x^2} + k^2\beta|A|^2A = 0 . \tag{3}$$

Three coefficients [v_g, v_g' ($\equiv \partial v_g/\partial k$), and β] in this equation are functions of E_0, σ_0, and k (or ω). We have already seen that we can adjust E_0 so that v_g is zero.

As we will discuss in Sec. III, Eq. (3) has the following properties: (i) The wave described in (2) is unstable with respect to modulation in both amplitude and phase, and "bright" envelope solitons may be formed when $\beta v_g' > 0$. (A bright soliton is an amplitude peak.) (ii) If $\beta v_g' < 0$, then the modulational instability does not appear, and the initial amplitude perturbation eventually breaks into "dark" solitons which are stable amplitude depressions. We will show that both of these cases are experimentally accesible in the electron–liquid-helium system.

There are a few particular combinations of k and E_0 where Eq. (3) is not valid because of the perturbation scheme we employ. We will also discuss the wave evolution in these particular cases in Sec. IV. We then extend our theory to discuss two-dimensional waves of the form

$$a(x,y,t) = A(x,y,t)\exp(ikx - i\omega t) . \tag{4}$$

It will be shown in Sec. V that such a wave is unstable with respect to the modulation in both x and y directions, when the wave number is large enough, so that the surface tension determines the properties of the wave. After the modulational instability has reached a large amplitude, the modulated waves may collapse. Finally, we present parameters and an idea related to the experimental studies in Sec. VI.

II. DERIVATION OF ONE-DIMENSIONAL NONLINEAR SCHRÖDINGER EQUATION

In this section, we consider a one-dimensional wave packet propagating in the x direction on the electron-charged surface of an incompressible liquid with depth z_0. The wave propagation is governed by the Laplace equation

$$\Delta\psi = 0 \tag{5}$$

for the velocity potential $\psi(x,z,t)$ subject to the

boundary conditions

$$\psi_z = 0 \tag{6}$$

at the bottom of liquid $z = -z_0$,

$$\psi_z = a_t + \psi_x a_x \tag{7}$$

at the surface of liquid $z = a(x,t)$, and

$$\psi_t + \tfrac{1}{2}(\nabla\psi)^2 + ga = (1/\rho)(\sigma\phi_z - \sigma_0\phi_{0z}) + (\alpha/\rho)a_{xx}(1 - \tfrac{3}{2}a_x^2) \quad \text{at } z = a(x,t). \tag{8}$$

Here $\sigma(x,t)$ is the surface-electron charge density, $\phi(x,z,t)$ the electrostatic potential, and ϕ_0 the potential when there is no surface displacement, $a = 0$. We choose the equilibrium surface at $z = 0$. The suffixes x, z, and t indicate partial derivatives with respect to those variables. The velocity of the liquid is derived from $\vec{v} = \nabla\psi$. As compared to the description of waves on water,[10,11] Eq. (8) has additional terms due to the electrical force on the electrons and to the surface tension which is usually taken to be small when one considers long wavelength waves but becomes the most important effect when the wavelength is short. To describe the electrical force term appearing in Eq. (8), we need a few more equations which are discussed in the latter half of this section.

Our first task is to express ψ_t and $\nabla\psi$ in terms of a and its derivatives by employing the solution of the Laplace equation (5). Let us introduce an operator,

$$\tilde{P} = -i(\partial/\partial x).$$

Then the solution of Eq. (5) satisfying the boundary condition (6) is given by

$$\psi(x,z,t) = \frac{\cosh[(z+z_0)\tilde{P}]}{\cosh z_0 \tilde{P}} f(x,t), \tag{9}$$

where $f(x,t) = \psi(x,0,t)$. Combining Eqs. (7) and (9) we find

$$\frac{\sinh[(a+z_0)\tilde{P}]}{\cosh z_0 \tilde{P}} \tilde{P} f(x,t) = a_t + \psi_x a_t. \tag{10}$$

This equation enables us to express ψ_x, ψ_z, and ψ_t at $z = a$ in terms of a and it's derivates, if we assume that $|ak| \ll 1$. The explicit expressions for ψ_x etc. are listed in Appendix A. Substitution of these expressions into Eq. (8) yields an equation for the surface displacement a.

We are interested in the evolution of a quasi-monochromatic wave or wave packet of the form given in Eq. (2). This fundamental wave component interacts with the second-harmonic component appearing at frequency 2ω and wave number $2k$ and the zero-frequency component which changes much more slowly compared to $\exp(ikx - i\omega t)$. As long as $|ak| \ll 1$, the interactions with the third- and higher-harmonic components can be neglected because they are higher-order effects. We therefore assume that the perturbation is written

$$a = \epsilon[A\exp(ikx - i\omega t) + A^*\exp(-ikx + i\omega t)] + \epsilon^2[B\exp(i2kx - i2\omega t) + B^*\exp(-i2kx + i2\omega t) + C]. \tag{11}$$

Here, $\epsilon (\ll 1)$ is an expansion parameter, and A, B, and C are slowly varying functions of x and t, so that both $|A_x/kA|$ and $|A_t/\omega A|$ are the order of magnitude of ϵ.

By using the above perturbation scheme we intend to derive an equation for the envelope function $A(x,t)$ rather than $a(x,t)$. To do so, we expand ψ_x, ψ_z, and ψ_t in a series of harmonics:

$$\begin{bmatrix}\psi_x\\ \psi_z\\ \psi_t\end{bmatrix} = \sum_{n=0}\begin{bmatrix}\psi_{xnk}(x,t)\\ \psi_{znk}(x,t)\\ \psi_{tnk}(x,t)\end{bmatrix}\exp[in(kx - \omega t)] + \text{c.c.} \tag{12}$$

Here the subscript nk stands for nth harmonic component. By using expressions for ψ_x, ψ_z, and ψ_t, Eqs. (A2), (A3), and (A4), we can write these harmonic components in terms of A, B, and C. The explicit expressions are listed in Appendix A. Substituting these expressions into Eq. (8), we obtain an equation for the first harmonic,

$$-\left(\omega + i\frac{\partial}{\partial t}\right)^2 A + 2k\omega^2 BA^* + 2k^2\omega^2|A|^2 A = -g\left(k - i\frac{\partial}{\partial x}\right)A + \frac{1}{\rho}\left(k - i\frac{\partial}{\partial x}\right)(\sigma\phi_z)_k - \frac{\alpha}{\rho}\left(k - i\frac{\partial}{\partial x}\right)^3 A, \tag{13}$$

and for the second harmonic,

$$-(2\omega^2/k)B + \omega^2 A = -gB - 4k^2(\alpha/\rho)B + (1/\rho)(\sigma\phi_z)_{2k}, \tag{14}$$

in the deep-liquid limit; $|kz_0| \to \infty$. These two equations yield the nonlinear equation for A in a closed form if $\sigma\phi_z - \sigma_0\phi_{0z}$ is written in terms of A and B.

We now need to describe the electrical force term appearing in Eqs. (13) and (4) in terms of a. The surface distortion modifies the electron density σ, so that it changes the electrostatic potential $\phi(x,z,t)$ which is described by the Poisson's equation

$$\Delta\varphi = 4\pi\sigma\delta(z - a). \tag{15}$$

The confining electric field E_0 applied in the z di-

rection allows electrons to move only along the liquid surface. Since both the period and the damping time of electron plasma oscillations are much shorter than the oscillation period of ripplons,[12] the inertia and the friction term appearing in the equation of motion of electrons can be neglected, so that we have

$$(\hat{x}\cos\theta+\hat{z}\sin\theta)\cdot\vec{E}=0 \quad \text{at } z=a, \tag{16}$$

where $\hat{x}$ and $\hat{z}$ are unit vectors in the x and z direction, and

$$\tan\theta=a_x. \tag{17}$$

Equation (15) indicates that the electric field $\vec{E}$ is perpendicular to the liquid surface. As a sheet of charge appearing in the Poisson's equation creates a discontinuous electric field, we use the averaged electric field

$$\vec{E}=-\tfrac{1}{2}(\nabla\phi^{+}+\nabla\phi^{-}) \quad \text{at } z=a(x,t) \tag{18}$$

in (16). Here, ϕ^{+} and ϕ^{-} are the potential above and below the surface, which are solutions of the Poisson's equation, $\Delta\phi=0$. In order to simplify the problem, we put metallic walls at $z=\pm z_0$. The Poisson's equation is then subject to the conditions

$$\phi_x=0 \quad \text{at } z=\pm z_0 \tag{19}$$

and

$$\phi^{+}=\phi^{-} \quad \text{at } z=a(x,t). \tag{20}$$

With the boundary condition (19) the solution of Eq. (15) is

$$\phi^{\pm}=\frac{\sinh|(z_0+z)\tilde{P}|}{\sinh z_0\tilde{P}}\,h^{\pm}(x,t)-E_0^{\pm}z. \tag{21}$$

The second term of this solution comes from the external field which is modified by the unperturbed surface charge σ_0. The averaged external field is obtained from $E_0=\frac{1}{2}(E_0^{+}+E_0^{-})$. Our purpose is to express $h^{\pm}$ in Eq. (21) in terms of $a(x,t)$. This can be done if we employ a series expansion

$$h^{\pm}(x,t)=\sum_{n=1}^{\infty}h^{\pm(n)}, \tag{22}$$

where $h^{(n)}$ are functions of $O(a^n)$. Using Eqs. (16)–(18) and (20) we can connect ϕ^{+} and ϕ^{-} at $z=a$. After some lengthy algebra, the connection of the two solutions yields

$$\begin{aligned} h^{\pm(1)}&=E_0^{\pm}a,\\ h^{\pm(2)}&=E_0^{\pm}a(\tilde{P}\tilde{T}a),\\ h^{\pm(3)}&=\tfrac{1}{2}E_0^{\pm}\{a^2a_{xx}+2a[\tilde{P}\tilde{T}a(\tilde{P}\tilde{T}a)]\}. \end{aligned} \tag{23}$$

Here $\tilde{T}\equiv\coth z_0\tilde{P}$. The potential can now be written in terms of a.

The calculation of σ is straightforward if we employ

$$(\hat{z}\cos\theta-\hat{x}\sin\theta)\cdot(\nabla\phi^{+}-\nabla\phi^{-})=-4\pi\sigma\cos\theta \quad \text{at } z=a, \tag{24}$$

which is obtained from (15) by integrating over a closed surface enclosing the infinitesimal electron layer. We find σ in terms of a by substituting Eqs. (21)–(23) into (24). In the limit of $|kz_0|\to\infty$, the electrical interaction terms appearing in Eqs. (13) and (14) are given by

$$\begin{aligned} (\sigma\phi_z)_k&=[\sigma\tfrac{1}{2}(\phi_z^{+}+\phi_z^{-})]_k\\ &=\frac{1}{2\pi}\Big\{[(2\pi\sigma_0)^2+E_0^2]\Big(k+i\frac{\partial}{\partial x}\Big)A\\ &\quad-4E_0(2\pi\sigma_0)k^2A^{*}B-2k^3E_0^2|A|^2A\\ &\quad+2k^3(2\pi)^2|A|^2A\Big\}+O(\epsilon^4) \end{aligned} \tag{25}$$

and

$$(\sigma\phi_z)_{2k}=(1/\pi)[(2\pi\sigma_0)^2+E_0^2]kB+O(\epsilon^3). \tag{26}$$

We now have the amplitude of the second harmonic

$$B=[2k\omega^2/(4\omega^2-\omega_{2k}^2)]A^2, \tag{27}$$

where

$$\omega_{2k}=\left(2gk-\frac{2[E_0^2+(2\pi\sigma_0)^2]}{\pi\rho}k^2+\frac{8\alpha}{\rho}k^3\right)^{1/2}$$

is the eigenfrequency at a wave number $2k$. The equation governing the first harmonic is

$$iA_t-\frac{1}{2\omega_k}A_{tt}+iv_gA_x+\tfrac{1}{2}\Big(v_g'+\frac{v_g'}{\omega_k}\Big)A_{xx}+k^2\beta|A|^2A=0. \tag{28}$$

The coefficients are given by

$$\begin{aligned} \omega_k^2&=gk-\frac{(2\pi\sigma_0)^2+E_0^2}{2\pi}k^2+\frac{\alpha}{\rho}k^3,\\ v_g&=\frac{\partial\omega_k}{\partial k},\quad v_g'=\frac{\partial^2\omega_k}{\partial k^2}, \end{aligned} \tag{29}$$

and

$$\beta=-\frac{\omega_k}{2}\left[\frac{2\omega_k^2}{4\omega_k^2-\omega_{2k}^2}\left(1+\frac{2k^2\sigma_0E_0}{\rho\omega_k^2}\right)+\left(1-\frac{3\alpha k^3}{4\rho\omega_k^2}\right)+\frac{k^2[E_0^2-(2\pi\sigma_0)^2]}{2\pi\rho\omega_k^2}\right]. \tag{30}$$

If the wave-packet variation is slower than the carrier frequency ω_k, then we have $A_{tt}\simeq v_g^2A_{xx}$, so that we obtain Eq. (3) from Eq. (28). In Sec. III, we discuss the equation for a normalized amplitude:

$$iF_t+iv_gF_x+\tfrac{1}{2}v_g'F_{xx}+\beta|F|^2F=0, \tag{31}$$

where

$$F(x,t) = kA(x,t) .$$

If we neglect the surface tension and the electrical interaction effect, i.e., if we set $\alpha = \sigma_0^2 = E_0^2 = 0$, then Eqs. (29)–(31) agrees with the results of the nonlinear deep-water wave theory.[11]

III. MODULATIONAL INSTABILITY AND SOLITONS

The uniform amplitude wave

$$F = F_0 \exp(i\beta |F_0|^2 t) \tag{32}$$

is a solution of Eq. (31). The exponential factor is indicative of a nonlinear frequency shift. Depending on the sign of $v_g'\beta$, this uniform wave can be both stable and unstable with respect to an envelope perturbation.[13] One can easily show that a small perturbation δF and δG, written in the form

$$F = \exp(i\beta |F_0|^2 t)[F_0 + \delta F \exp(iKx - i\Omega t) + \delta G \exp(-iKx - i\Omega^* t)] , \tag{33}$$

with the definition

$$a = (F/k) \exp(ikx - i\omega_k t) + \text{c.c.} ,$$

evolves according to the dispersion relation

$$(\Omega - Kv_g)^2 = \tfrac{1}{4} v_g'^2 K^4 - v_g'\beta |F_0|^2 K^2 . \tag{34}$$

We find from (34) that the perturbation grows, i.e., the uniform wave is unstable with respect to the amplitude and phase modulation when $v_g'\beta > 0$. We call this a modulation instability. The maximum growth rate

$$\gamma_m \equiv (\mathrm{Im}\Omega)_{\max} = |\beta| \, |F_0|^2 \tag{35}$$

is obtained when

$$K^2 = (2\beta/v_g') |F_0|^2 \equiv K_m^2 . \tag{36}$$

The uniform wave is stable, when $v_g'\beta < 0$.

In Fig. 3, we show stable and unstable regions in the $E_0^2 - k$ plane. We have neglected σ_0 appearing in Eqs. (29) and (30). The modulational instability grows in the regions labeled U. The label S indicates the stable regions. We are especially interested in the behavior of the system near to $v_g = 0$. Here, the real part of Ω vanishes, indicating that the unstable modulation does not propagate. The curve $v_g = 0$ is also plotted in Fig. 3. We find that the modulational instability grows at point A on the dispersion curve in Fig. 2. We have a stable wave at point B. In order to show the k dependence of a maximum growth rate γ_m, we plot β in Fig. 4 as a function of k. The singularity of β appearing at $k = (\rho g/2\alpha)^{1/2}$ is due to the resonance of the second-harmonic wave [see Eq. (27)].

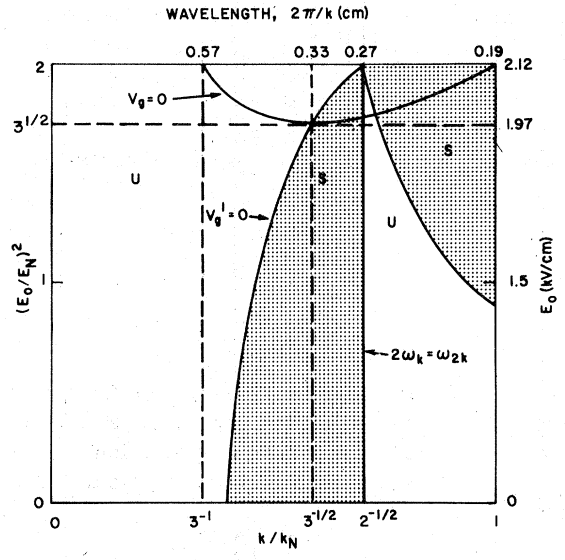

FIG. 3. Modulationally stable (labeled S) and unstable (labeled U) regions in E_0-k plane.

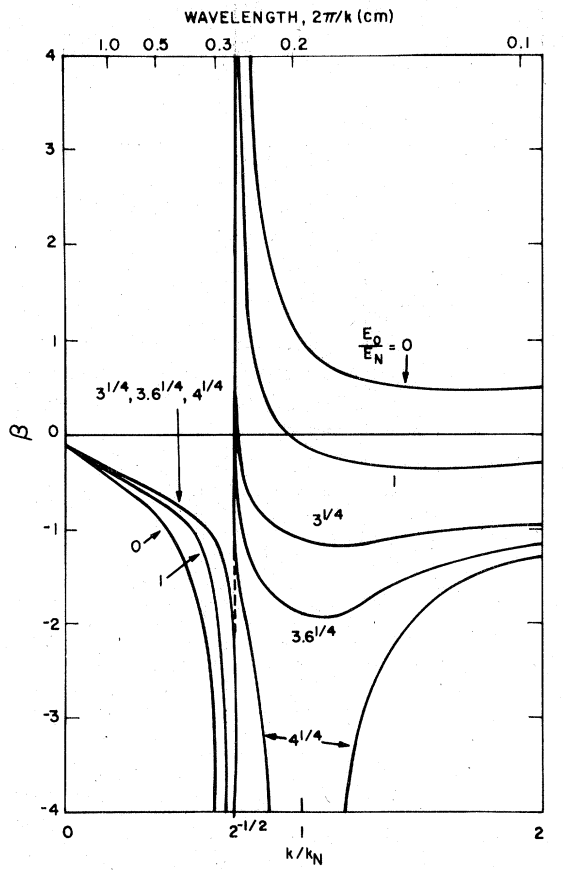

FIG. 4. Coefficient β of the nonlinear term in Eq. (31) as a function of wave number with E_0 as a parameter.

We are also interested in the case when k is very large, so that only the surface tension determines the properties of the waves. From Eqs. (29) and (30) we have

$$v_g' = \tfrac{3}{4}\,(\alpha/\rho)^{1/2}k^{-1/2}$$

and (37)

$$\beta = \tfrac{1}{8}\,(\alpha/\rho)^{1/2}k^{3/2},$$

if $k^2 \gg (2E_0^2/\pi\alpha)^2$ and $\rho g/\alpha$. We again find modulational instability. If the system length L is larger than the instability growth length v_g/γ_m, then the modulational instability grows to large amplitude. From (35) and (37) this criterion turns out to be

$$|F_0|^2 \gg 12/kL\,. \tag{38}$$

The modulational instability occuring at these short wavelengths has to be considered when one carries out an experiment such as the detection of two-dimensional electron lattice[14] by using resonant excitation of ripplons.

It is well know that Eq. (31) has stationary-state solutions which can be expressed in terms of Jacobian elliptic functions. Soliton solutions, exhibiting the dynamical balance between nonlinear and dispersion effects, belong to these types of solutions.

When $v_g'\beta < 0$, we have "dark" solitions characterized by

$$F(x,t) = F_0 \tanh\,[(-\beta\,|F_0|^2/v_g')^{1/2}(x - v_g t)] \times \exp(i\beta\,|F_0|^2 t)\,. \tag{38}$$

These disturbances have an amplitude dip and a phase jump moving with the group velocity. In this modulationally stable case, the arbitrary perturbation around the uniform equilibrium amplitude given by (32) is described by the Korteweg-deVries equation.[15] The properties of the Korteweg-deVries equation are well known.[16] The initial arbitrary perturbation breaks into dark solitons.

When $v_g'\beta > 0$, we have "bright" solitons,

$$F = F_0\,\mathrm{sech}\,[(\beta\,|F_0|^2/v_g')^{1/2}(x - v_g t)] \times \exp(i\tfrac{1}{2}\beta\,|F_0|^2 t)\,. \tag{40}$$

Since the width of this soliton is about the same as K_m^{-1} given in Eq. (36), solitons are created in the nonlinear stage of the modulational instability.[17] Zakharov and Shabat[18] have found exact solutions of the nonlinear Schrödinger equation. They have shown that an arbitrary wave packet disintegrates into a number of solitions. They also have predicted some interesting properties of these solutions such as bound-state oscillations. In this case solitons behave as if they were bound to each other (see also Ref. 4).

The long-time behavior of solitons has not been observed experimentally presumably due to dissipation in the experimental system. We expect the system considered here is suitable for observing the nonlinear interactions.

IV. SPECIAL CASES

There are three special combinations of E_0 and k for which Eq. (31) is not valid. One particular case is when $v_g' = 0$. The lowest-order dispersion term to be appeared in Eq. (31) is then $(\frac{1}{6})(\partial^3\omega/\partial k^3)F_{xxx}$. However, this third-order derivative term introduces only a small shift of the velocity of the envelope and does not affect the stability of the envelope.

Another more interesting case is when $k = (\rho g/2\alpha)^{1/2}$ for all E_0. At this particular wave number, the second-harmonic wave satisfies the linear dispersion relation, $2\omega_k = \omega_{2k}$ [see Eq. (27)]. Therefore, the amplitude of the second-harmonic mode becomes the same order of magnitude as the fundamental-mode amplitude, and the dominant nonlinear interaction occurs only between these two modes. As we show in Appendix B, the spatially uniform waves exhibit amplitude oscillations in time. If the second-harmonic wave is excited initially, then the decay instability[19] produces sidebands and may cause spatial amplitude modulation on the fundamental mode. The fundamental-mode wave packet emits waves at the second harmonic because the group velocity of these two modes are different.

The final special case is the marginal state for the interchange instability, i.e., $\omega_k = 0$ which occurs when $E_0^2 = 4\pi(g\rho\alpha)^{1/2} - (2\pi\sigma_0)^2$ and $k = (\rho g/\alpha)^{1/2}$. Although our analysis fails to be valid in this case, the large negative value of β (positive nonlinear frequency shift) near $\omega_k = 0$ implies that finite-amplitude effects tend to stabilize the interchange instability (see Fig. 4).

V. TWO-DIMENSIONAL WAVE MODULATION AND COLLAPSE

So far, we have considered only the case when the modulation wave vector is parallel to the carrier wave vector. The problem of two-dimensional modulation is interesting because it relates to the collapse phenomenon of the wave packet.[5] We derive an equation describing two-dimensional wave-packet evolution in Appendix C. The final result

$$i(F_t + v_g F_x) + \tfrac{1}{2}[v_g' F_{xx} + (v_g/k)F_{yy}] + \beta\,|F|^2 F = 0 \tag{41}$$

indicates that the dispersion term is anisotropic. Here we have choosen the carrier wave vector k to be in the positive x direction.

It can be shown that a two dimensional wave packet shrinks in all directions if $\beta v_g' > 0$ and $v_g v_g' > 0$. We have already seen that the dynamical balance between the nonlinear and the dispersion effects keeps the shape of the one-dimensional soliton given by Eq. (40). However, if the wave packet shrinks in both x and y directions, then the dispersion effect can not stop the contraction because the amplitude increases more rapidly than in the case of one-dimensional contraction, so that the nonlinear term always dominates over the dispersion term in (41). This collapse phenomenon is described by a self-similar solution of Eq. (41).[6] The collapse continues until higher-order nonlinear and dispersion terms become effective. If $\beta v_g' > 0$ or $\beta v_g > 0$ and $v_g v_g' < 0$, then the wave packet contracts in one direction (say, in the x direction) and expands in the other direction (say, in the y direction).

The conditions $\beta v_g' > 0$ and $v_g v_g' > 0$ is achieved in the right-hand-side unstable region in Fig. 3. When the wave number is very large, the coefficients of the dispersion and nonlinear terms are given by Eq. (37) and $v_g/k = \frac{3}{2}(\alpha/\rho k)^{1/2}$. All these coefficients are positive, indicating that the occurrence of modulational instability at large wave number gives rise to collapse of the modulated waves in the nonlinear stage of the instability. From the self-similar solution obtained in Ref. 6, we find the condition for the collapse to occur in a finite size system is also given by Eq. (38).

VI. PARAMETERS AND SUGGESTED EXPERIMENT

We summarize numerical values of the quantities appearing in our theory. In Figs. 2–4 we have employed quantities defined by

$$\omega_N^2 = g(\rho g/\alpha)^{1/2}\,, \qquad k_N = (\rho g/\alpha)^{1/2}\,, \qquad E_N^2 = 2\pi(\rho g\alpha)^{1/2}\,, \tag{42}$$

to normalize the frequency, the wave number, and the confining electric field, respectively. If we put $\rho = 0.13$ g/cm^3 and $\alpha = 0.12$ dyn/cm for liquid helium at 4.2 °K, then the above normalizing quantities are: $\omega_N/2\pi = 28$ Hz, $\lambda_N = 2\pi/k_N = 0.19$ cm, and $E_N = 1.5$ kV/cm. We have neglected σ_0 in Figs. 2–4, because $(2\pi\sigma_0/E_N)^2 = 3.6\times 10^{-3}$, if we use practical surface-electron density of 10^8 cm^{-2} [see Eqs. (29) and (30)].

We find in Fig. 2 that $v_g = 0$ appears at $\lambda = 2\pi/k = 0.6$ cm when E_0 is in the range between 1.97 and 2.12 Kv/cm. The frequency $\omega/2\pi$ is always about 10 Hz. This wave is unstable with respect to the modulational instability, and the wave energy does not propagate out from the system. Yanof has found experimentally that a large fluctuation at about 10 Hz easily appears if one does not carefully isolate the system from external vibrations.[20] Another wave with $v_g = 0$ appears at $\lambda \simeq 0.2$ cm, where the envelope is stable.

Since we can control the dispersion relations by changing E_0, the following experiment is possible. We first set E_0 below 1.97 Kv/cm and launch a wave packet at an end of the system. After the wave packet reaches the middle of the system, we suddenly increase E_0 to a value above 1.97 Kv/cm. If we choose initial carrier frequency properly, the wave packet does not escape from the system. We can now observe the long-time behavior of solitons. When the frequency is above a few kHz, the dispersion relation is determined only by the surface tension. We then can observe collapse of the wave packet.

ACKNOWLEDGMENT

Authors thank A. L. Simons for his numerical calculations and appreciate discussions with A. Hasegawa, P. M. Platzman, and A. W. Yanof.

APPENDIX A: EXPRESSIONS OF ψ_x, ψ_z, ψ_t, AND FOURIER COEFFICIENTS

We expand the left-hand side of (10) in a power series of $a\tilde{P}$ and find

$$\tilde{P}f = \cot a\tilde{P}[a_t + \psi_x a_x - a\tilde{P}\tilde{T}(a_t + \psi_x a_x) - \tfrac{1}{2}a^2\tilde{P}^2 a_t + a\tilde{P}\tilde{T}a_t]\,, \tag{A1}$$

where $\tilde{T} \equiv \coth z_0\tilde{P}$ and $\tilde{P} \equiv -i(\partial/\partial x)$. Differentiating (9) with respect to x and using (A1), we obtain

$$\psi_x = i\tilde{T}[(1 - a\tilde{P}\tilde{T})a_t + ia_x\tilde{T}a_t] + ia\tilde{P}a_t\,. \tag{A2}$$

From (7) and (A2), we have

$$\psi_z \simeq a_t + ia_x\tilde{T}a_t\,. \tag{A3}$$

Equations (A2) and (A3) are correct up to $O(a^2)$. Differentiating (9) with respect to time, we also have

$$\psi_t = \frac{\sinh[(a+z_0)\tilde{P}]}{\cosh z_0\tilde{P}}\,\frac{1}{\tilde{P}}\,(\tilde{P}f)_t \simeq \frac{1}{\tilde{P}}\,\tilde{T}\,\frac{\partial}{\partial t}\{[1 - a\tilde{P}\tilde{T} + (a\tilde{P}\tilde{T})^2]a_t - \tfrac{1}{2}a^2\tilde{P}^2 a_t + (1 - a\tilde{P}\tilde{T})\psi_x a_x\} + a\,\frac{\partial}{\partial t}(a_t - a\tilde{P}\tilde{T}a_t + \psi_x a_x) + \tfrac{1}{2}a^2\tilde{P}\,\frac{\partial}{\partial t}\,Ta_t\,, \tag{A4}$$

which is correct up to $O(a^3)$.

The coefficients appearing in Eq. (12) are calculated by using Eqs. (A2)–(A4). We find

$$\begin{aligned}
&\psi_{xk} = \epsilon\omega A + O(\epsilon^2)\,,\\
&\psi_{zk} = -i\omega\epsilon A + O(\epsilon^2)\,,\\
&\psi_{x2k} = (2\omega B - k\omega A^2)\epsilon^2 + O(\epsilon^4)\,,\\
&\psi_{z2k} = (-2i\omega B + ik\omega A^2)\epsilon^2 + O(\epsilon^4)\,,\\
&\psi_{x0} = 2k\omega\,|A\,|^2\epsilon^2 + O(\epsilon^4)\,,\\
&\psi_{z0} = O(\epsilon^3)\,,\\
&\left(k + i\,\frac{\partial}{\partial t}\right)\psi_{tk} = -\left(\omega + i\,\frac{\partial}{\partial t}\right)^2\epsilon A - 2k\omega^2 BA^*\epsilon^3\\
&\qquad\qquad + 2k^2\omega^2\,|A\,|^2 A\epsilon^3 + O(\epsilon^4)\,,
\end{aligned} \tag{A5}$$

and

$$2kA_{t2k} = 2k\omega^2 A^2 - 2\omega^2 B\,.$$

APPENDIX B: RESONANT INTERACTION BETWEEN FIRST AND SECOND HARMONICS

When the second-harmonic component $(2\omega_k, 2k)$ satisfies the linear dispersion relation, i.e., when $2\omega_k = \omega_{2k}$, the fundamental mode and the second-harmonic mode strongly interact. This resonant interaction occurs when $k = (\rho g/2\alpha)^{1/2}$. The amplitude of the second harmonics then becomes the same order of magnitude as the fundamental-mode amplitude. As the coupling to the other components is nonresonant, the set of equations

$$\begin{aligned}
&i(A_t + v_{g1}A_x) + GBA^* = 0\,,\\
&i(B_t + v_{g2}B_x) + \Delta\omega B + HA^2 = 0
\end{aligned} \tag{B1}$$

describe the wave evolution. Here, v_{g1} and v_{g2} are the group velocity of the fundamental and the second-harmonic waves $G = -k\omega_k - 2\sigma_0 E_0 k^3/\omega_k$, $H = k\omega_k$, and $\Delta\omega = (4\omega_k^2 - 2\omega_{2k}^2)/2\omega_k$. The definition of A and B are given in Eq. (11).

We consider the spatially uniform solution of (B1) with the initial condition $A(t=0) = A_0$ and $B(t=0) = 0$. Taking into account the conservation law, $H|A|^2 + G|B|^2 = H|A_0|^2$, we eliminate B from (B1) and have

$$i\Delta\omega A_t + A_{tt} - 2HG|A|^2 A + HG|A_0|^2 A = 0\,. \tag{B2}$$

We define a function $s = A\exp(i\Delta\omega t/2)$ and obtain

$$s_{tt} + (\tfrac{1}{4}\Delta\omega^2 - HG|A_0|^2)s + 2HG|s|^2 s = 0\,. \tag{B3}$$

The solution of (B3) under the condition $s(t=0) = A_0$ and $S_t|_{t=0} = 0$ is written in terms of Jacobi's elliptic function

$$|s|^2 = |A_0|^2[\mathrm{cn}^2(\Omega t; k)/\mathrm{dn}^2(\Omega t; k)] = |A|^2\,. \tag{B4}$$

From the conservation law, the intensity of the second-harmonic wave becomes

$$|B|^2 = |A_0|^2\{1 - [\mathrm{cn}^2(\Omega t; k)/\mathrm{dn}^2(\Omega t; k)]\}\,. \tag{B5}$$

These solutions show the amplitude oscillation of the both modes.

APPENDIX C: DERIVATION OF THE TWO-DIMENSIONAL WAVE-PACKET EQUATION

For a two-dimensional surface distortion, the surface-tension term should be replaced by $\alpha(a_{xx} + a_{yy})$ in the linear regime. The linearized equation corresponding to Eq. (8) becomes

$$\psi_t + ga = (1/\rho)(\sigma\phi_z - \sigma_0\phi_{0z}) + \alpha\Delta_\perp a\,, \tag{C1}$$

where $\Delta_\perp = \partial^2/\partial x^2 + \partial^2/\partial y^2$. On the other hand, the three-dimensional solution of Eq. (5) is obtained simply by replacing the operator $\tilde{P}$ by $(-\Delta_\perp)^{1/2}$ in Eq. (9). f is now a function of x, y, and t. By repeating the procedures we have employed to derive Eq. (13) we obtain

$$\begin{aligned}
-\psi_{tt} = &-g(-\Delta_\perp)^{1/2}\psi + (\alpha/\rho)(-\Delta_\perp)^{3/2}\psi\\
&+ (1/\rho)(-\Delta_\perp)^{1/2}(\sigma\phi_z - \sigma_0\phi_{0z})\,.
\end{aligned} \tag{C2}$$

The equation of motion of the electrons on the surface is modified to be

$$m\frac{d\vec{v}_e}{dt} = -et\cdot\mathbf{E}\hat{t} + e(\hat{t}\times\hat{z})\cdot\mathbf{E}(\hat{t}\times\hat{z})/|\hat{t}\times\hat{z}|\,. \tag{C3}$$

Here, $\vec{v}_e$, m, $-e$, are the velocity, mass, and charge of the electron, and $\hat{t}$ is the tangential unit vector along the maximum gradient direction of the liquid surface, which is expressed by

$$\hat{t} = \cos\theta\cos\eta\,\hat{x} + \cos\theta\sin\eta\,\hat{y} - \sin\eta\,\hat{z}\,, \tag{C4}$$

where $\theta = \tan^{-1}(a_x^2 + a_y^2)^{1/2}$, $\eta = \tan^{-1}(a_y/a_x)$. We neglect the electron inertia and from (C3) and (C4) we obtain

$$\begin{aligned}
&\cos\theta\cos\eta\,\phi_x + \cos\theta\sin\eta\,\phi_y - \sin\eta\,\phi_z = 0\,,\\
&\sin\eta\,\phi_x - \cos\eta\,\phi_y = 0\,.
\end{aligned} \tag{C5}$$

The three-dimensional solution of the Poisson's equation is again the same as Eq. (21), provided $\tilde{P}$ is replaced by $(-\Delta_\perp)^{1/2}$. Using (C5) and the potential continuity condition (20), we obtain an expression of $h^\pm(x, y, t)$:

$$h^\pm = E_0^\pm a\,. \tag{C6}$$

In the linear regime, the surface electron charge density is given by

$$\sigma - \sigma_0 = (-\phi_z^+ + \phi_z^- - E_0^+ + E_0^-)/4\pi\,. \tag{C7}$$

Combination of Eqs. (21), (C6), and (C7) yields

$$\begin{aligned}
&\tfrac{1}{2}[\sigma(\phi_z^+ + \phi_z^-) + \sigma_0(E_0^+ + E_0^-)]\\
&\qquad = (1/2\pi)[(2\pi\sigma_0)^2 + E_0^2](-\Delta_1)^{1/2}a\,.
\end{aligned} \tag{C8}$$

The two-dimensional wave equation is obtained by substituting (C8) into (C2):

$$a_{tt} = -g(-\Delta_\perp)a - (1/2\pi\rho)[(2\pi\sigma_0)^2 + E_0^2]\Delta_\perp a - \alpha(-\Delta_\perp)^{3/2}a \ . \quad \text{(C9)}$$

To derive the two-dimensional wave-packet equation, we combine (C9) and the nonlinear term in Eq. (31). Choosing the carrier wave vector along the positive x direction, we obtain final Eq. (41). A fully nonlinear three-dimensional calculation from the starting equations gives us the same result.

---

*Present address: Institute for Laser Engineering, Osaka University, Suita, Japan.

[1]A. C. Scott, F. Y. F. Chu, and D. W. McLaughlin, Proc. IEEE 61, 1443 (1973).

[2]A. Hasegawa and F. Tappert, Appl. Phys. Lett. 23, 142 (1973).

[3]E. Fermi, J. Pasta, and S. Ulam, in *Empirco Fermi Collected Papers* (Univ. of Chicago, Chicago, 1965), Vol. II, p. 977; N. J. Zabusky and M. D. Kruskal, Phys. Rev. Lett. 15, 240 (1965).

[4]G. Roskes, Phys. Fluids 19, 766 (1976); H. C. Yuen and B. M. Lake, *ibid.* 19, 767 (1976). The bound-state oscillation was originally found by Zakharov and Shabat (see Ref. 18).

[5]V. E. Zakharov, Zh. Eksp. Teor. Fiz. 62, 1745 (1972) [Sov. Phys.-JETP 35, 908 (1972); L. M. Degtyarev, V. E. Zakharov, and L. I. Rudakov, *ibid.* 68, 115 (1975) [*ibid.* 41, 57 (1975)].

[6]V. E. Zakharov and V. S. Synakh, Zh. Eksp. Teor. Fiz. 68, 940 (1975) [Sov. Phys.-JETP 41, 465 (1975)].

[7]T. B. Benjamin and J. E. Feir, J. Fluid Mech. 27, 417 (1967); H. C. Yuen and B. M. Lake, Phys. Fluids 18, 956 (1975); H. Ikezi, K. Nishikawa, and K. Mima, J. Phys. Soc. Jpn. 37, 766 (1974); H. Ikezi, R. J. Taylor, and D. R. Baker, Phys. Rev. Lett. 25, 11 (1970); H. Ikezi, Phys. Fluids 16, 1668 (1973); R. Hirota and K. Suzuki, J. Phys. Soc. Jpn. 28, 1366 (1970).

[8]K. Mima, H. Ikezi, and A. Hasegawa, Phys. Rev. B 14, 3953 (1976).

[9]L. P. Gorkov and D. M. Chernikova, Zh. Eksp. Teor. Fiz. Pis'ma Red. 18, 119 (1973) [JETP Lett. 18, 68 (1973)].

[10]M. J. Lighthill, Proc. R. Soc. A 299, 28 (1967); W. D. Hayes, Proc. R. Soc. A 320, 187 (1970).

[11]V. H. Chu and C. C. Mei, J. Fluid Mech. 41, 873 (1970); H. Hashimoto and H. Ono, J. Phys. Soc. Jpn. 33, 805 (1972); A. Davey and K. Stewartson, Proc. R. Soc. A 338, 101 (1974).

[12]C. C. Grimes and G. Adams, Phys. Rev. Lett. 36, 145 (1976).

[13]T. B. Benjamin, Proc. R. Soc. A 299, 59 (1967); G. B. Witham, J. Fluid Mech. 27, 399 (1967).

[14]P. M. Platzman and H. Fukuyama, Phys. Rev. B 10, 3150 (1974); R. W. Hockney and T. R. Brown, J. Phys. C 8, 1813 (1975).

[15]T. Taniuti and N. Yajima, J. Math. Phys. 10, 1369 (1969).

[16]C. S. Gardner, J. M. Green, M. D. Kruskal, and R. M. Miura, Phys. Rev. Lett. 19, 1095 (1967).

[17]V. I. Karpman and E. M. Krushkal, Zh. Eksp. Teor. Fiz. 55, 530 (1968) [Sov. Phys.-JETP 28, 277 (1969)].

[18]V. E. Zakharov and A. B. Shabat, Zh. Eksp. Teor. Fiz. 61, 118 (1971) [Sov. Phys.-JETP 34, 62 (1972)].

[19]D. DuBois and M. Goldman, Phys. Rev. Lett. 14, 544 (1965); K. Nishikawa, J. Phys. Soc. Jpn. 24, 916 (1968).

[20]A. W. Yanof (private communication).